STUDY OF LOW DIMENSIONAL TUNGSTEN OXIDE BY ANODIZATION AND SOL-GEL METHODS

by

CHAI YINGQI

Thesis submitted in fulfillment of the requirements
for the degree of
Doctor of Philosophy

June 2018

ACKNOWLEDGEMENT

First of all, I would like to thank my supervisor, Dr. Yam Fong Kwong, and my co-supervisor, Prof. Zainuriah Hassan, for their easygoing supervision and guidance throughout this project. Their advice, dedication and energy to me are appreciated.

I would also like to show my gratitude to the lab assistants of Institute of Nano-Optoeletronics Research and Technology as well as the School of Physics of University Sains of Malaysia (USM). Their help in providing a convenient working environment and experimental equipments allowed me to run my experiments smoothly. Besides, I would also like to thank my colleagues and other researchers from NOR lab for the great discussions and suggestions.

Finally and mostly, I would also like to thank my family and friends for their support and motivation.

TABLE OF CONTENTS

LIST OF TABLES

Page

LIST OF FIGURES

Page

LIST OF ABBREVIATIONS

CVD	Chemical vapour deposition
EC	Electrochromic
FTO	Fluorine doped tin oxide
GPTS	2-(2,3 epoxypropxy)propyl-trimethoxysilane
HFCVD	Hot filament chemical vapour deposition
IDE	Interdigitated electrode
IPA	Isopropanol
IPCE	Incident photon to electron conversion efficiency
ITO	Indium tin oxide
IUPAC	International Union of Pure and Applied Chemistry
MPECVD	Microwave plasma-enhanced chemical vapour deposition
NPs	Nanoparticles
OLED	Organic light emitting diodes
PA	Polyacrylic acid
PAA	Porous anodic alumina
PCB	Printed circuit board
PEC	Photoelectrochemical

PET	Polyester
POA	Poly(o-anisidine)
PMAPTAC	Poly-[3-(methacrylamino)propyl]trimethyl ammonium chloride
PPy	Polypyrrole
PTA	Peroxopolytungstic acid
PTN	2,4-pentanedione
PVA	Poly(vinylalcohol)
RH	Relative humidity
RTP	Room temperature (~25°C)
SMOLED	Small molecule organic light emitting diodes
SMU	Source measure unit
TCTA	4,4',4"-tris(carbazol-9yl)-triphenylamine
TEG	Tetraethyleneglycol
TEOS	Tetraethoxysilane
TiO_2	titanium dioxide
Vol.	Volume
WO_3	Tungsten trioxide
$WO_{\leq 3}$	Tungsten oxide
Wt.	Weight

PENGAJIAN TUNGSTEN OKSIDA DIMENSI RENDAH DENGAN KAEDAH PENGANODAN DAN SOL-GEL

ABSTRAK

Low dimensi tungsten oksida ($WO_{\leq 3}$) dapat menarik perhatian penyelidikan sebab aplikasi ia sebagai peranti elektrokromik, sensor gas, peranti fotokatalis untuk pembahagian molekul air, sel solar secara pencelupan dan sensor kelembapan. Penggunaan tungsten oksida sebagai peranti permukaan-sensitif memerlukan fabrikasi tungsten oksida yang berkos efektif dan berkawalan morfologi. Kaedah penganodan dan sol-gel menawarkan cara-cara sintesis nanostruktur tungsten trioksida (WO_3) yang mudah. Akan tetapi, pengajian tentang penggunaan kaedah penganodan dan sol-gel untuk mengfabrikasi nanostruktur WO_3 adalah tidak mencukupi. Tesis ini mengkaji penggunaan kaedah penganodan dan sol-gel untuk pembentukan nanostruktur WO_3. Kesan-kesan parameter penganodan (elektrolit, voltan, tempoh, dan suhu) dan parameter sol-gel (isipadu asid, tempoh penuaan, dan kadar pencampuran asid) pada ciri-ciri WO_3 disamping ciri-ciri sensor fotoelektrokimia dan kelembapannya juga diperiksa masing-masing. Penganodan dalam electrolit yang berbeza menghasilkan nanostruktur yang berbeza. Lapisan nanoliang (~400 nm) dapat dibentukkan dalam asid oksalik sementara lapisan nanopiring (>1 μm) telah ditunjukkan oleh penganodan dalam HCl dan H_2SO_4. Daripada keputusan eksperimen, mekanisme penumbuhan nanoliang dan nanopiring telah dicadangkan. Pengukuran arus foto menunjukkan bahawa struktur nanoliang mempunyai keputusan pengukuran arus foto yang lebih baik berbanding dengan struktur nanopiring. Dalam penumbuhan WO_3 dengan sol-gel teknik, nanopiring

dapat dibentukkan. Penggunaan isipadu asid yang lebih tinggi, tempoh penuaan yang lebih pendek, dan kadar pencampuran asid yang lebih lambat didapati akan mengecilkan saiz nanopiring. Sampel yang ditumbuhkan dengan isipadu acid yang tinggi (>40 ml) menunjukkan struktur kristal tungsten trioksida terhidrat (WO_3•$2H_2O$ and WO_3•H_2O) dan WO_3. Sensor kelembapan jenis rintangan yang sangat sensitif dapat difabrikasikan dengan penyalutan sampel WO_3 ke atas interdigital elektrod yang diperbuat sendiri. Kepekaan sensor kelembapan yang tinggi (~190000) telah diperolehi oleh sampel yang mempunyai dimensi nanopiring yang kecil, susunan krystal yang bagus dan pemukaan kumpulan-oxo.

STUDY OF LOW DIMENSIONAL TUNGSTEN OXIDE BY ANODIZATION AND SOL-GEL METHODS

ABSTRACT

Low dimensional tungsten oxides ($WO_{\leq 3}$) have attracted considerable research attention due to potential applications such as electrochromic devices, gas sensors, photocatalysts for water splitting, dye-sensitized solar cells and humidity sensors. The use of tungsten oxide for surface-sensitive device applications requires cost-effective fabrication of tungsten oxide with controllable morphological property. Both anodization and sol-gel methods offer facile ways to synthesize nanostructured tungsten trioxide (WO_3). However, inadequate works have been done to employ anodization and sol-gel techniques for the fabrication of nanostructured WO_3. In this thesis, investigations of the use of anodization and sol-gel methods for the formation of nanostructured WO_3 are presented. The effects of anodization parameters (electrolyte, voltage, duration, and temperature) and sol-gel parameters (acid volume, ageing duration, and mixing rate) on the properties of the WO_3 as well as their photoelectrochemical and humidity sensing properties were also examined respectively. Anodization in different electrolytes resulted in different nanostructures. Nanoporous layer of ~400 nm could be formed in oxalic acid while nanoplates layer of >1 μm were demonstrated by anodization in HCl and H_2SO_4. From our experimental results, growth mechanisms of nanopores and nanoplates were both proposed. Photocurrent measurements revealed that nanoporous structure had better photoelectrochemical response as compared to the nanoplate structure. For the fabrication of WO_3 by sol-gel method, nanoplates could be formed. Higher

volume of acid, shorter ageing duration and slower mixing rate were found to decrease the size of nanoplates. As-grown sample in high acidic volume (>40 ml) could exist in crystalline structure of hydrated tungsten trioxide ($WO_3 \bullet 2H_2O$ and $WO_3 \bullet H_2O$) and WO_3. Resistive type humidity sensors with high sensitivity were successfully fabricated by coating WO_3 samples on the self-synthesized interdigitated electrode. High humidity sensitivity of ~190000 was achieved by the sample with smaller nanoplates, good crystallinity and surface oxo-group.

CHAPTER 1: INTRODUCTION

1.1 Introduction

This chapter gives a general overview of tungsten oxide by briefly introducing the potential applications of tungsten oxide as well as various fabrication methods. Fabrication techniques based on anodization and sol-gel methods will be discussed, followed by review of the fields and problem statements. In addition, the objectives and the novelties of the project are presented.

1.2 Why Tungsten Oxide

Tungsten oxide ($WO_{\leq 3}$) is an n-type semiconductor with the indirect bandgap of (2.60 – 3.25 eV) [1, 2]. Apart from the stable and popular tungsten trioxide (WO_3), tungsten oxides could exist as oxygen deficient oxides as $WO_{2.92}$, $WO_{2.9}$, $WO_{2.83}$, $WO_{2.77}$, $WO_{2.72}$, $WO_{2.67}$ and $WO_{2.63}$ due to the non-stoichiometeric property of WO_3 [1]. It has been reported that tungsten oxide has high chemical stability at appropriate pH value, good electric conductivity ranging from 10 to 10^{-4} Scm^{-1} depending on the stoichiometry, modulated optical property where the physical color can change from yellow to dark blue with the presence of external stimuli (applied voltage and reducing gases) and charge-storage/delivery properties due to the valence change between W^{6+} and W^{5+} [1-4]. Owing to these properties, tungsten oxide has attracted considerable research attention particular for the green and renewable energy related applications (e.g. electrochromic window [5], dye-sensitized solar cell [6], photocatalyst for water splitting [7]) and other applicants (e.g. gas sensor [8] and humidity sensor [9]).

Since the invention of electrochromic device by Deb in 1969 [10], tungsten oxide has become one of the most promising materials for the study of electrochromic property which can change the transparency of windows by applying voltage [11]. Electrochromic windows could help save energy consumption in buildings by controlling the transparency of the windows. According to the research, > 1 % of the United States annual energy consumption, or more than $10 billion energy waste could be saved by using electrochromic windows [12].

From the literature, Zheng and co-authors have demonstrated the fabrication of dye-sensitized solar cell based on WO_3 [6]. At the forefront of research on photovoltaic devices, dye-sensitized solar cell has the advantage of low level requirement of material processing and the simplicity of cell assembly. Dye-sensitized solar cells based on titanium dioxide could achieve efficiency approaching 12 % [13]. Tungsten oxide, a more stable material in the exposure of strong acids and carrier mobility (10.2 - 2.8 cm^2/Vs) with the range of titanium dioxide, is believed to have potential to act as photoanode for electron transport material in dye sensitized solar cells with acceptable efficiency [6].

Yafeng et al. [14] and Berger et al. [15] have demonstrated the photoelectrochemical water splitting property of WO_3 for hydrogen production. This application allows the conversion of solar energy directly to the hydrogen gas which could be used as renewable energy with zero pollution in the process of energy generation.

1.3 Fabrication methods of nanostructured tungsten oxide

Considering the applications of tungsten oxide, fabrications of low dimensional tungsten oxide have been attracting great scientific interests. Compared with their bulk tungsten oxide counterparts, nanostructured tungsten oxide has high surface aspect ratio which could significantly enhance their sensitivity. For example, with the estimated porosity of 65 %, Berger et al. demonstrated that four-fold increase of the photocurrent was achieved by the nanoporous film compared to the thick film [15]. Besides, nanomaterials could have different physical, chemical and electronic properties from the thick film due to quantum confinement effect. For instance, increase of the band gap energy was detected with the reduction of the grain size [16]. Owing to these advantages, various techniques used for the fabrication of nanostructured tungsten oxide have been developed to improve the performance of their applications. Appendix A shows the table of the various techniques used for fabrication of nanostructured tungsten oxides.

Nguyen et al. fabricated tungsten oxides nanowires with the length of a few micrometers and diameters of 90-1000 nm using thermal evaporation technique where the pressure and temperature were controlled at 10^{-2} -10 Torr and 950 - 1050 °C [17]. The improvement of NO_2 gas sensing performance was demonstrated and they pointed out that this could be due to the formation of nanowires structure. Zhang et al. grew platinum-activated tungsten oxides with the grain sizes of ~30 nm using radio frequency sputtering in 0.2 Pascal [18]. Their results showed high gas sensor response of 4 s in 200 ppm H_2 at 220 °C. Tesfamichael et al. synthesized tungsten oxide nanoparticles with the diamaters of 2.6 -12 nm using electron beam evaporation technique operating at 4 kV in the pressure of 10^{-5} -10^{-4} Pa and tested for

the gas sensing response [19]. They attributed the high sensitivity (450) of the gas sensor in 5 ppm NO_2 to the small grain sizes and high porosity of the film.

These fabrication methods of low-dimensional tungsten oxides require sophisticated machines like sputtering machine, electron gun, and thermal evaporation system with the vacuum system and often operating at high temperature condition which will increase the production cost for the device applications. Electrochromic device has been synthesized using sputtering machine and commercialized for the automobile window, however, it can't be utilized for the window of the building because of the the limitation of the sputtering system to fabricate the film in large size. As a result of these, attempts to fabricate nanostructured tungsten oxide have been made by other methods, such as sol-gel and anodization which are able to grow nanostructure in large scale and size with only simple experiment tools and setups such as chemical, electrolyte, power supply and glassware. This motivates our present work to synthesize nanostructured tungsten oxide by anodization and sol-gel techniques.

1.3.1 Anodization

Anodization is a very simple and cheap process employed in fabricating nanostructure which requires only electrochemical cell consisting of power supply, electrolyte, target sample as anode and cathode. When the power is turned on in the electrochemical cell, oxygen ions from the electrolyte will react with anode to form metal oxide while hydrogen ions will receive the electrons from the inert cathode to form hydrogen gas. Anodization process has been first employed as a method to grow thick protective oxide layer on the metal to prevent it from corrosion. It was then used as a process to grow nanostructure for porous anodic alumina by using

suitable parameters [20]. After research for 5 decades, anodic growth of alumina could achieve tunable size (pore diameter: 25 -420 nm; cell size: 25 -42 nm; thickness of the porous layer: 350 nm -80 μm) and shape (close-packed array of hexagonal cells with a cylindrical central) [21-25]. Owing to the abundancy of alumina and well control of the porous structure, anodic growth alumina has been widely used as a template to assist the growth of nanostructure of other materials [26, 27].

Following the successful to grow porous alumina, huge efforts have been exerted to study fabrication of nanostructure by anodization method on other valve metals, especially on titanium [28-31]. Grimes et al. synthesized titanium dioxide nanotube using hydrofluoric acid [32]. However, they failed to control the size of nanotubes where only tube lengths of ~250 nm were achieved which were too short for applications as the photoelectrohemical device and dyed-sensitized cell. After enormous efforts were devoted, significant improvements have been made. By using different electrolytes such as mixing of fluoride based electrolytes with buffer electrolytes (sodium fluoride), polar organic electrolytes (ethylene glycol) or using non-fluoride based electrolytes (hydrochloric acid, hydrogen peroxide and perchloric acid) to control the pH, water content of the solution and concentration of the acid, precisely controllable and self-ordered nanoscale could be achieved [33-36]. Anodization has a huge advantage for the fabrication of nanostructure where desired dimension of nanotubes of titanium dioxide or nanopores of alumina could be obtained by tuning the anodization parameters (e.g. applied source, type of electrolyte, electrolyte concentration/temperature, and duration). Great achievements to form self-ordered nanostructure on alumina and titanium dioxide have given

researcher confidence and driven them to explore the formation of nanostructured WO_3 using anodization method.

1.3.2 Sol gel

Sol-gel process is a wet chemical method for the fabrication of solid inorganic polymers/ceramic (silicon oxide[37], titanium oxide[38], tungsten oxide[39] and etc[40, 41]) from the transformation of liquid precursors to a sol and gel through hydrolysis and condensation processes. Sol-gel method requires only chemicals reactants and glass wares which are free of any sophisicated and high cost machine. This offers a low cost and simple technique to produce ceramic and complex inorganic materials at low temperatures while the conventional way to produce ceramic requires high temperature condition at their melting point.

Sol-gel method was first introduced in 1845 for the synthesis of hydrous silica which could be used to produce fibers and optical lenses [42]. In spite of early discovery, sol-gel chemistry only attracted interest in 20 century because of the deficiency of the sol-gel technology at that moment where long drying period of 1 year was required to avoid fracture of silica gels [43, 44]. As time goes by, knowledge and technologies on the sol-gel science were gained and improved gradually where ultralight aerogels had been invented in 1932 [45] while homogeneous powders of aluminum oxide, silicon oxide, titanium oxide, zirconium oxide were successfully prepared in 1950 [44]. It was until 1960, sol-gel science has attracted great interest of studies [44, 46, 47]. With the ability to control the size and morphology, sol-gel technology was extended into many other materials like oxide, hydroxides, sulfides to prepare glass, ceramic fibers, ITO coating and etc [48-52]. Owing to the nature of sol-gel technique where sols are made from the

interconnected small molecules starting from precursors, the homogeneity of the solution could be achieved at molecular level. In addition, the purity and properties (crystal phase and refractive index) can also be controlled by choosing refined precursors and types of ligands of the precursors [53].

1.4 Current research and problem statements

Fabrication by anodization and sol-gel methods are both facile and inexpensive techniques to fabricate nanostructured WO_3. As the material properties are dependent on the synthesis condition, as-grown WO_3 samples with these different techniques have different properties and particular interest of applications.

Development of the formation of WO_3 by anodization method is shown in Appendix B. Fabricating on the conductive tungsten metal contact, anodic growth of WO_3 is widely studied for their application as photoelectrochemical response [14, 15, 54] but not for gas sensing and electrochromic applications which require non-conductive or transparent substrate. As the photoelectrochemical device requires illumination of sun light on the film to function, control of the morphological property of the sample plays a crucial role. Majority of the anodic growth of WO_3 films used fluoride based electrolytes and result in thin porous layer (< 500 nm) [14, 15, 28, 55, 56]. To improve the performance of the device application, control of the thickness of the nanostructured layer is essential. As shown by Shankar et al., increase of the thickness of nanotube array of titanium dioxide from 8.2 μm to 14.4 μm increase the photoconversion efficiency from 9.88 to 14.42% [57]. However, further increase the length of the nanotubes will decrease the photoconversion efficiency due to the recombination of the photogenerated charges. In the attempt to increase the thickness of nanostructured layer of WO_3, Watcharenwong et al.

employed viscous solutions as electrolyte in the anodization [54]. While this method was found to be workable for the anodization of titanium to control the thickness and length of the tubes, they reported no significant improvement of the thickness in the case of WO_3.

Yang et al. successfully synthesized WO_3 with the nanostructured layer thickness of ~2 μm by anodization [58]. However, concentrated hydrofluoric acid (40%) and phosphoric acid (85%) were utilized in order to form the thick nanostructured layer. Lee et al. fabricated nanoporous WO_3 with the thickness of the porous layer up to 9 μm using potassium hydrogen phosphate in glycerol at 80 - 100 °C [59]. Although they successfully grew thick porous layer, they still failed to control the size of the pores and erosion of the wall of the pores. No notable improvement of the morphological properties of the anodic growth of WO_3 was reported in recent year. We suggest that this is due to the inadequate understanding of the mechanism of the anodic growth of WO_3. Further work is necessary to control the morphological property of the nanostructured WO_3 for device applications. Exploration on the formation of nanostructured WO_3 using non-fluoride based electrolyte could be beneficial to control the morphological property of the WO_3 as the formation of nanostructures utilizing fluoride based electrolytes have yet to achieve the goal while attempts to use non-fluoride based electrolytes for the formation of self-ordered titanium dioxide nanotubes have been proven to be successful.

Fabrication of WO_3 by sol-gel method on the other hand, often studies for their electrochromic properties [60-64]. (Appendix C shows the development of the growth of WO_3 by sol-gel method.) For example, Soliman et al. improved the electrochromic properties by obtaining a stable solution with the addition of oxalic acid, H_2O_2 [65] or using different precursors ($WOCl_4$) [61]. In addition, lithium

based compound was added to improve the bleaching process while polystrene microspheres template was used to produce high density pores [66]. Apart from that, gold particle was incorporated to improve faster diffusion and charge transfer rates [64].

The study of the formation of nanostructure WO_3 using sol-gel method or exploration of the sol-gel synthesized WO_3 for the other applications such as photoelectrochemical (PEC) water splitting device [67], gas sensor [68], gasochromic device [69], OLED [70] and humidity sensor [71] has not been emphasized. In the research on the formation of nanostructure by sol-gel method, effects of different acids, pHs, mixing rates on the spin coater, and humidity of the drying environments on the morphological properties of the WO_3 have been studied and examined for their NO_2 gas sensing properties [39, 68]. However, the research on the formation of nanostructured WO_3 from sol-gel method is still inadequate where the detail study of the effects of the sol-gel parameters such as type of the precursor, concentration of the precursor, mixing rate, ageing duration, additive and temperature of synthesis on the formation of nanostructure are remain unclear. To the best of our knowledge, only Dai et al. utilized sol-gel-made WO_3 to synthesize humidity sensor [71]. However, their research focused on the archictecture of the humidity sensor which was integrated with micro-heater and inverting amplifier circuit on chip manufactured using complementary metal oxide semiconductor and micro-electromechanical systems (CMOS-MEM) while no study was made on the effect of the nanostructure on the sensing properties. Sundaram et al. and Patil et al. fabricated humidity sensor based on WO_3 but their research focused on the compositions of lead, zinc or poly(*o*-anisidine) to the purchased WO_3 to improve the

sensitivity of the sensor [72, 73]. None of them has investigated the effect of the properties of the nanostructured WO_3 on the humidity sensor.

1.5 Research Objectives

1. To study the effect of anodization parameters using non-fluoride based electrolytes on the morphological property of WO_3 and their photoelectrochemical property.

2. To investigate and examine the effect of sol-gel parameters on the growth of low-dimensional WO_3.

3. To explore and develop the application of sol-gel fabricated WO_3 as humidity sensor.

1.6 Research Novelties

1. Fabrication of thick nanoplate structure by anodization method using H_2SO_4 and HCl.

2. Proposed growth mechanisms of the WO_3 nanopores and nanoplates formed by anodization method.

3. Dimensionality control of nanostructured WO_3 by tuning sol-gel parameters.

4. Development of extremely high sensitivity humidity sensor based on pristine WO_3 grown by sol-gel method.

1.7 Outline of Thesis

Chapter 1 shows applications of tungsten oxide, fabrication methods of nanostructured tungsten oxide including anodization and sol-gel methods, review of

the fields, problem statements, research objectives and the novelties of the research works.

Chapter 2 describes the fundamental properties of tungsten oxide, the theories of the growth of tungsten oxide by anodization and sol-gel methods. In addition, theories and overview of their applications as photoelectrochemical cell and humidity sensor are also presented.

Chapter 3 presents the experimental procedure to grow WO_3 by both anodization and sol-gel methods. Experimental procedures to fabricate photocatalytic water splitting device and humidity sensor are also described.

Chapter 4 discusses the fabrication and characterization of the WO_3 samples grown by anodization method. Their photocatalytic properties are also examined.

Chapter 5 covers the results and discussion of the sol-gel-made WO_3 and their humidity sensing property.

Finally, chapter 6 provides a summary of the current research and suggestion for future research.

CHAPTER 2: LITERATURE REVIEW AND RESEARCH BACKGROUND

2.1 Introduction

This chapter provides information of the fundamental properties of tungsten oxide. Literature reviews and theories of the fabrication of tungsten oxide by anodization and sol-gel technniques are discussed. Apart from these, theories and background of the applications of tungsten oxide as photoelectrochemical water splitting and humidity sensor are also presented.

2.2 Fundamental properties of tungsten oxide

Tungsten oxide is an n-type semiconductor which has a 2.60- 3.25 eV indirect bandgap [1, 2] and 10 to 10^{-4} Scm^{-1} electrical conductivity where their bandgap and electrical conductivity could be largely varied by crystallinity, grain size, grain boundary, stoichiometry/oxygen vacancy and film thickness [1, 2, 74-80]. For example, the large bandgap of 3.25 eV reported for the WO_3 in the amorphous stage with large grain size can be reduced to 2.62 eV in the crystalline structure [81]. Besides the bandgap of WO_3 can also be decreased with an increase of oxygen vacancy [1] or a decrease in grain size [79]. On the other hand, electron mobility of WO_3 was reported to be 6.5 $cm^2V^{-1}s^{-1}$ [77], which has significantly improved to 40 $cm^2V^{-1}S^{-1}$ for the case of $W_{18}O_{49}$ with the oxygen vacancies acting as the donors [80].

WO_3 is formed by corner-sharing of WO_6 octahedra which could be arranged in the crystalline form with different tilting angles and rotation order as triclinic, monoclinic, orthorhombic, tetragonal, cubic and hexagonal phase, as shown in figure 2.1 [82]. Each of these phases is stable at the specific temperatures as shown in figure 2.1 which are partially reversible [83]. It should be noted that the change of

the phase does not suddenly happen at the distinct temperature [84] and the stability of the phase in the temperature as shown in figure 2.1 is reported for bulk WO_3, which could be varied for low dimensional WO_3 and fabrication techniques [85].

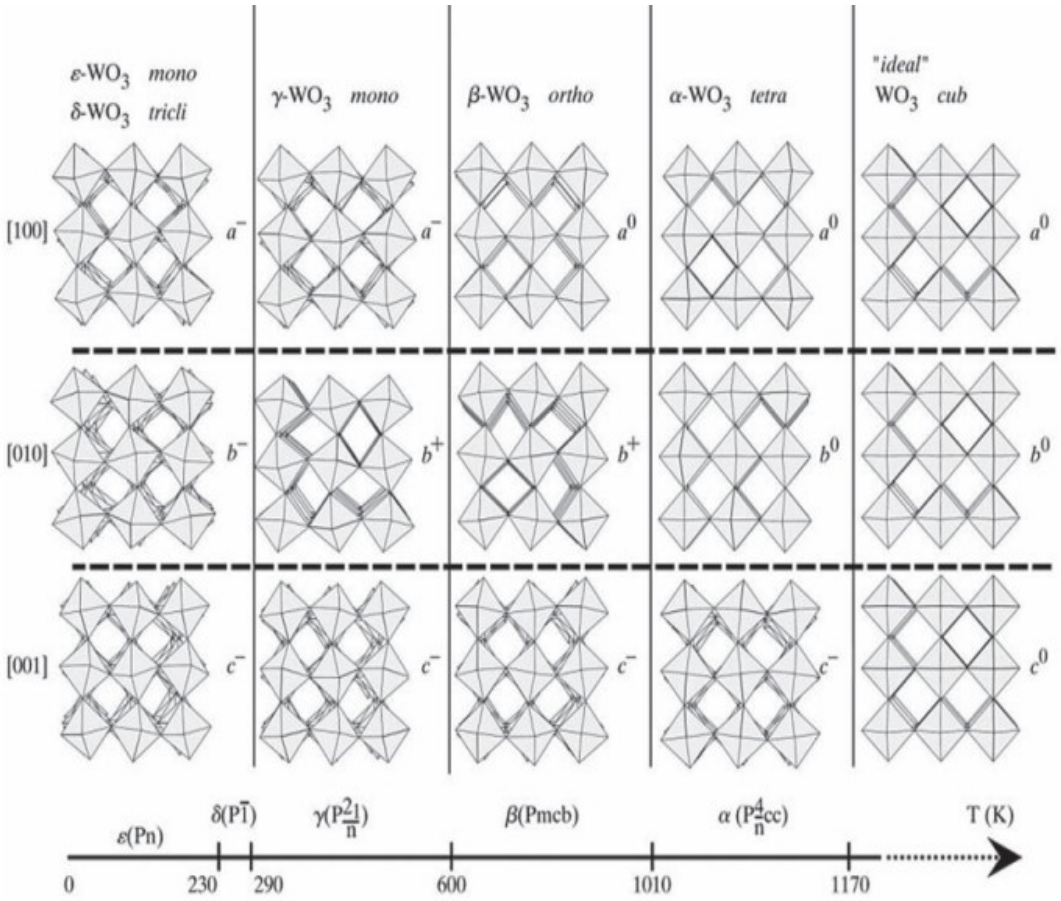

Figure 2.1 Stability of polymorphs of WO_3 at different temperatures. Source: Ref. [82].

Fabrications of tungsten oxides could result in WO_3, $WO_{x<3}$ (x = 2.92, 2.9, 2.83, 2.77, 2.72, 2.67 and 2.63) with oxygen vacancies and $WO_3 \bullet xH_2O$ (i.e. $WO_3 \bullet 2H_2O$, $WO_3 \bullet H_2O$, $WO_3 \bullet 0.33H_2O$) [1]. $WO_{x<3}$ are usually obtained by fabrication using thermal evaporation techniques or annealing of any form of tungsten oxide in oxygen deficient environment at high temperature [17, 86] while annealing in oxygen environment would result in WO_3 [87]. The presence of WO_x with oxygen vacancies could be attributed to the removal of oxygen from WO_3 by transforming the corner-

sharing WO_6 (figure 2.2(a)) to both corner- and edge-sharing structure (figure 2.2(b)), according to crystal-shear mechanism [88, 89]. These WO_x with the oxygen vacancies as a shallow donor have different properties as compared to WO_3 as discussed earlier.

$WO_3 \bullet xH_2O$ or hydrated tungsten oxides are usually formed by liquid related synthesis method (hydrothermal, sol-gel) which could transform to WO_3 by annealing [39, 90]. $WO_3 \bullet H_2O$ could be formed by substitution of one oxygen from the WO_6 octahedra by H_2O or by intercalation of H_2O between the sheets of the layered structure and not bonded to W^{6+} [91]. $WO_3 \bullet 2H_2O$ consists layers of octahedra similar to $WO_3 \bullet H_2O$. The intercalation of the second water molecule between the layers was found to increase the layer distance by ~23 % [92]. $WO_3 \bullet 0.33H_2O$ is formed by stacking layers of WO_6 octahedra where part of the oxygen atoms from WO_6 are replaced by W=O and W-$(OH)_2$ bonding [93]. $WO_3 \bullet xH_2O$ could be found in both amorphous and crystal phases [39].

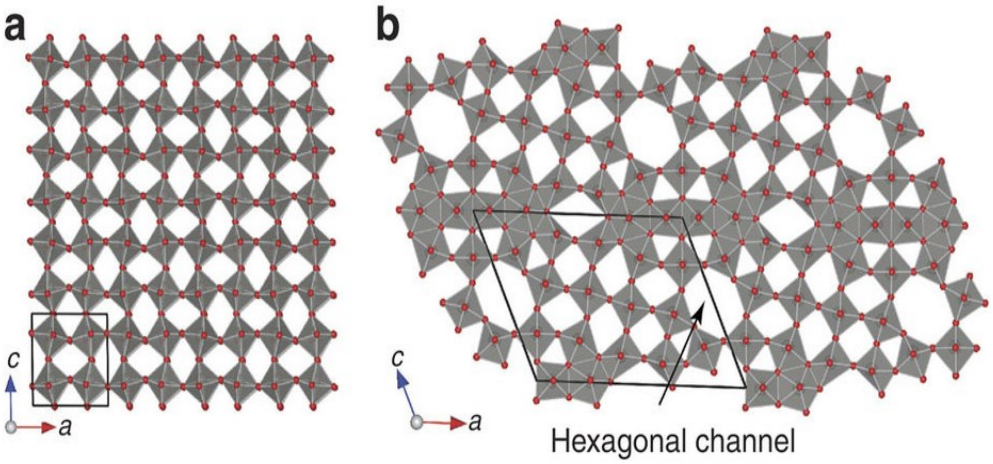

Figure 2.2 (a) Crystalline WO_3 structure with corner-sharing WO_6 octahedra layers. (b) $W_{18}O_{49}$ structure with both corner- and edge-sharing WO_6 octahedra layers. Source: Ref. [89].

2.3 Anodic growth mechanism of nanostructured WO_3

Formation of nanostructure through anodization method was first started on porous alumina and then applied to other valve metals such as titanium. After the research groups working on anodization of titanium have successfully grown titanium dioxide nanotubes, they applied this anodization technology on tungsten to form nanostructured tungsten oxide. The presence anodization technology for the formation of nanostructured WO_3 is still in the process of development and yet to be well documented. However, well studied anodization processes of WO_3 in different pHs were provided by Johnson et al. [45] and Anik et al.[94]. In this section, mechanism of the formation of nanostructured WO_3 are proposed by combining the general information of the formations of nanostructures by anodization from other valve metals (Al, Ti) and chemical dissolution mechanisms of WO_3 in the anodization process.

Generally, nanostructure formation from the anodization technique is usually driven by 3 processes: electrochemical oxidation, electrochemical dissolution and chemical dissolution [32]. When the power supply is turned on, both electrochemical oxidation (equation 2.1 and 2.2) and dissolution processes (equation 2.3) begin simultaneously in acidic condition [45, 95].

$$2W + 5H_2O \rightarrow W_2O_5 + 10H^+ + 10e^- \quad (2.1)$$

$$W_2O_5 + H_2O \rightarrow 2WO_3 + 2H^+ + 2e^- \quad (2.2)$$

$$W + 2H_2O \rightarrow WO_2^{2+} + 4H^+ + 6e^- \quad (2.3)$$

The strength of the electrochemical dissolution is affected by both the applied potential and the oxide barrier layer. Considering this, etching rate at the thin oxide

layer of the pit/holes is much higher than the the bulk oxide surface, resulting of the growth of the thickness of the porous layer [32]. The initial formation of small pits could be explained by the localized dissolution of the oxide layer [96].

After the formation of oxide layer, chemical dissolution also takes part to etch away the oxide layer other than electrochemical dissolution [97]. Unlike anodization of other metals (Al, Ti), chemical dissolution process of WO_3 is very complex due to the stoichiometry of WO_3 and various tungstate ions [94]. Chemical dissolution of WO_3 could be classified in three catagories: H^+ assisted, water molecules assisted and OH^- assisted chemical dissolution [94]. While all three types of chemical dissolutions could happen simultaneously, each of the processes is dominant in a specific pH value. Under high acidic condition, H^+ assisted chemical dissolution as shown in equation 2.4 is dominant while in less acidic condition, water molecules assisted dissolution is the main process as shown in equation 2.5 [94]. On the other hand, under high pH condition, OH^- assisted chemical process as shown in equation 2.6 is more dominant [94].

$$WO_3 + 2H^+ \rightarrow WO_2^{2+} + H_2O \tag{2.4}$$

$$WO_3 + H_2O \rightarrow H_2WO_4(aqueous) \tag{2.5}$$

$$WO_3 + OH^- \rightarrow WO_4^{2-} + H^+ \tag{2.6}$$

It is believed that the complicated chemical dissolution of WO_3 is the reason of the poor control of the morphology of anodic growth WO_3. In order to control the morphology of nanostructure, the electrochemical oxidation and dissolution as well as the chemical dissolution have to be well controlled. In the case of porous anodic growth alumina, electrochemical dissolution is dominant compared to chemical

dissolution where the effect of chemical dissolution could be ignored [32]. Rate of the field assisted dissolution at the pits is much higher than the bulk oxide layer due to the high field effect at thin oxide layer of the pit [98, 99]. This results in the continuous growth of the pit/pores, leading to the self-organized PAA with controllable thickness by tuning the potential, as shown in figure 2.3 [99].

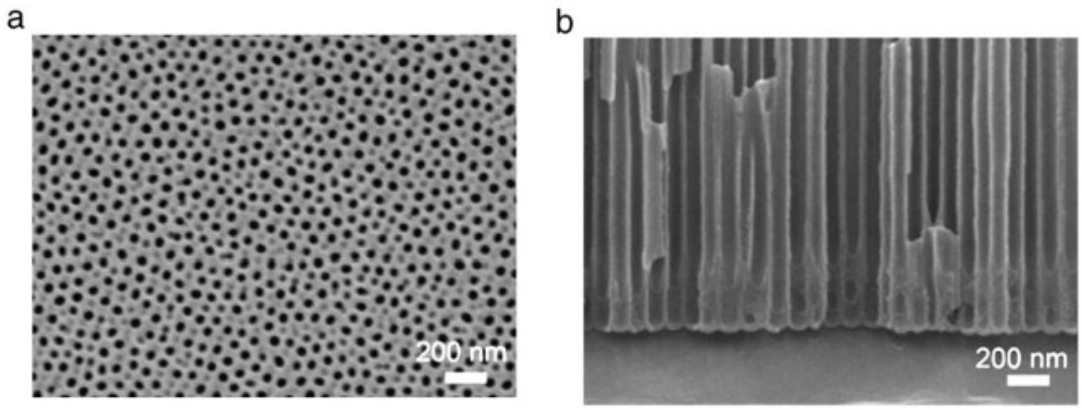

Figure 2.3 (a) Plane view and (b) cross section view of SEM images of anodic growth alumina in 0.5 M oxalic acid at 15 °C for 1h. Source: Ref. [99].

In the case of the anodic growth titanium dioxide nanotubes, the rate of chemical dissolution is comparable or even higher than the rate of electrochemical dissolution where chemical dissolution etches both the porous oxide layer and oxide barrier on the the film surface, hindering the growth of the porous layer thickness [97]. To control the chemical dissolution, high viscosity electrolytes like ethylene glycol and glycerol are employed to restrict the chemical dissolution at the oxide barrier on the film surface while allows the chemical dissolution at the pores, resulting in the self-organized nanotubes, as shown in figure 2.4 [100]. Considering the formation of thin porous layer (figure 2.5(b)) and the uncontrolled etching of the porous wall (figure 2.5, figure 2.6), it is believe that anodic growth WO_3 has higher chemical dissolution rate than the electrochemical dissolution rate [15, 58].

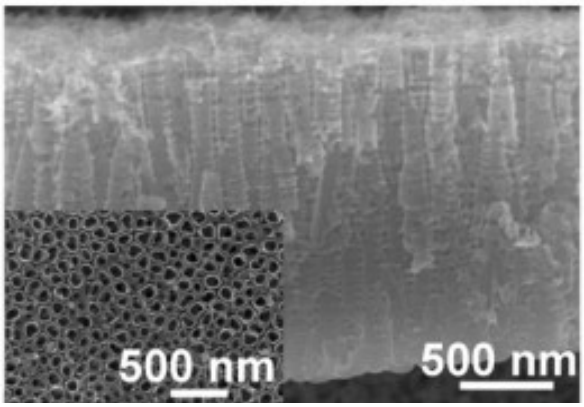

Figure 2.4 Cross sectional view of SEM image of titanium oxide nanotubes formed in mixture of glycerol and water (50:50 vol. %) + 0.5 wt. % NH_4F. Inset shows the corresponding plane view image. Source: Ref. [100].

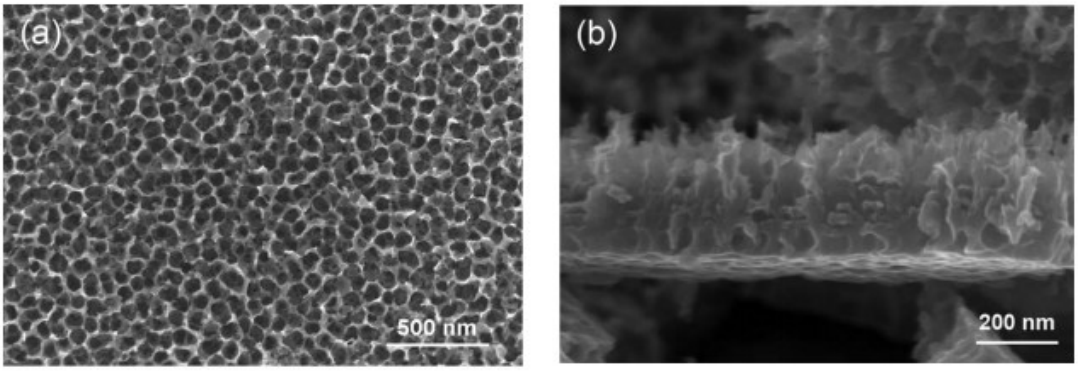

Figure 2.5 (a) Plane view and (b) cross sectional view SEM images of WO_3 grown in 0.5 wt % NaF + 1 M H_2SO_4. Source: Ref.[15].

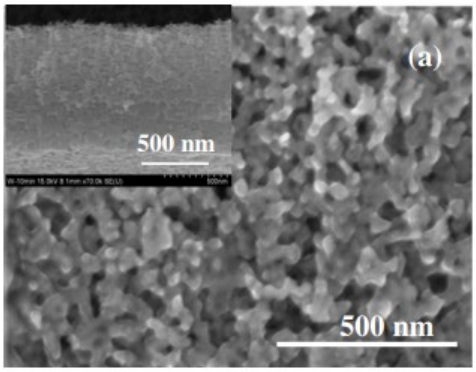

Figure 2.6 SEM image of WO_3 formed in H_3PO_4 + 8 M HF. Inset depicts the cross sectional image of the corresponding image. Source: Ref. [58].

Apart than the porous structure, platelet structure could also be attained due to the precipitation of the soluble tungstate charge (WO_2^{2+}). As described by Ng et al., with

the assistance of electric field and presence of water molecules, the saturated WO_2^{2+} in the suitable pH could precipitate on the W surface as shown in equation 2.7, 2.8 and 2.9 [95]. Formation of nanoplates by precipitation is also demonstrated by Widenkvist et al., in the chemical bath method [101].

$$WO_2^{2+} + 3H_2O \Leftrightarrow WO_3 \bullet 2H_2O + 2H^+ \quad (2.7)$$

$$WO_2^{2+} + 2H_2O \Leftrightarrow WO_3 \bullet H_2O + 2H^+ \quad (2.8)$$

$$WO_2^{2+} + H_2O \Leftrightarrow WO_3 + 2H^+ \quad (2.9)$$

2.4 Fabrication of WO_3 by sol-gel method

2.4.1 Type of precursors

Sol-gel-made WO_3 can be formed by five different types of precursors which are: 1) colloidal tungstic solutions (Na_2WO_4) [60, 102], 2) Peroxotungstic acid (PPTA/PTA) [103, 104], 3) tungsten hexachlorides (WCl_6) [53], 4) tungsten oxychloride ($WOCl_4$) [61], and 5) tungsten alkoxides [70].

Colloidal tungstic solution is usually formed by acidification of Na_2WO_4 (mixing with acid or passing through ion exchange resin). This precursor was firstly used in 1983 by Chemseddin to test for electrochromic property [60]. It is the most frequently used precursors to synthesize WO_3 by sol-gel method, however, formation of sol-gel using Na_2WO_4 precursor is not stable [102]. Unstable sol will transform to gel and precipitate very fast which is not suitable for electrochromic device [102]. To overcome this, stabilizing agents like oxalic acid, H_2O_2, acetic acid and alcohol are added into the solution [65, 102]. Owing to this deficiency, this precursor is replaced by WCl_6 and PPTA. Both WCl_6 and PPTA are inexpensive starting materials (PPTA could be formed by mixing of W powder with H_2O_2) which could form stable sol-gel

compared to Na_2WO_4 precursor. Fabrication of WO_3 from $WOCl_4$ is stable and shows good electrochromic properties [61]. However, it requires dry atmosphere and suffers from long term stability problem. Among all the precursors, tungsten alkoxide is the least studied precursor due to the high material cost and fast reaction with moisture [103].

2.4.2 Sol-gel process

There are 5 sol-gel processes, which are: 1) Mixing of precursors and formation of sol; 2) gelation; 3) ageing; 4) drying/syneresis; 5) dehydration and densification [44, 105]. The product of the sol-gel is highly dependent on the sol-gel process parameters, for example: selection of the type of precursors, ligands of the precursors, types of additive used, duration and condition of ageing and heat treatment temperature [44].

1) Mixing of precursors and formation of sol:

In sol-gel chemistry, precursor is the starting compound which comprises of two components (metal or metalloid bonds with number of ligands). At the first step, precursor is mixed with water at certain pH. This step leads to hydrolysis and condensation of the precursor, resulting in the formation of sol. Hydrolysis is a reaction involving the breaking of a bond in a molecule using water. For an example, hydrolysis of metal alkoxides is shown in equation 2.10 [105]:

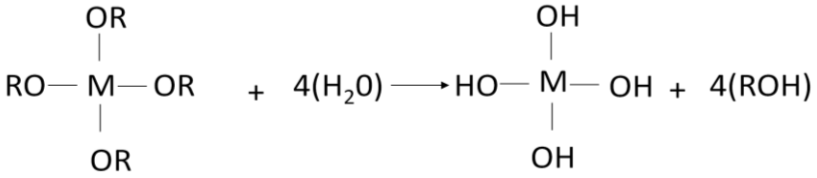

(2.10)

where M and R could be any metal/metalloid and ligand respectively. Hydrolyzed molecules can connect to each other in condensation reaction to liberate small molecules, as shown in equation 2.11 [105]:

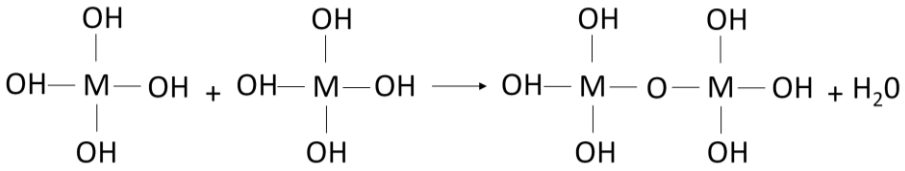

(2.11)

Through continuous hydrolysis and polycondensation reactions, M-O-M bonds interconnect with each other forming larger particles. As the particles size reach submicrometer size, sol is formed. According to IUPAC, sol is a colloidal suspension (solid particles with diameters of 1-1000 nm) in a liquid. Considering the small size of the sol, gravitational forces are negligible and the sols could move randomly in the solution according to Brownian motion.

2) Gelation:

Gel is a single giant cluster network which is formed from further condensation of several sols or polymers [105]. No change of bonding and latent heat is involved in gelation process. However, formation of gel could be easily recognized as the viscosity of the gel increase significantly from sol due to the large cluster network of gel, as shown in Appendix D. The structure of gel is determined by the hydrolysis and condensation processes [106].

3) Ageing:

Ageing allows the gel or the sample immerses in liquid for a time span, allowing further polycondensation and precipitation of the gel network which increases the thickness of interparticle necks and decreases the porosity [105].

4) Drying/Syneresis

Drying process expel the liquid from the gel/ precipitate. Drying process has to be controlled to prevent cracking due to the capillary stress[105].

5) Dehydration and densification

Dehydration process removes the hydroxyl bonds from the pore network by heat treatment [105].

2.5 Photoelectrochemical water splitting

Water splitting is the process to split water molecule to obtain both hydrogen and oxygen gases. It is currently received tremendous research focus because hydrogen is considered as unlimited source from water or renewable energy, which can replace our current fossil fuel to provide zero pollution fuel with high thermodynamic conversion efficiency. This solves the two of the main problems of our curent living issues: pollution and depletion of the fossil fuel.

Currently, hydrogen energy is mostly provided by coal gasification and biomass materials [107]. However, both of these methods produce byproducts of pollutant gases (CO_2, CH_4) [107] which is not desirable. Therefore, there is an urgent need to develop photoelectrochemical water splitting which is still in the research stage. Photoelectrochemical water splitting was first reported by Fujishima and Honda in 1972, which employs solar energy to split the water molecules in order to obtain hydrogen gas [108].

2.5.1 Principle and efficiency of photo-electrode water splitting

Figure 2.7 shows the experimental setup of the photoelectrochemical water splitting system based on n-type semiconductor photoelectrode [109]. The mechanisms of the photoelectrochemical water splitting process are also illustrated in the figure 2.7. There are three main steps for the photo-electrode water splitting to occur in photoelectrochemical cell (PEC) [109, 110]:

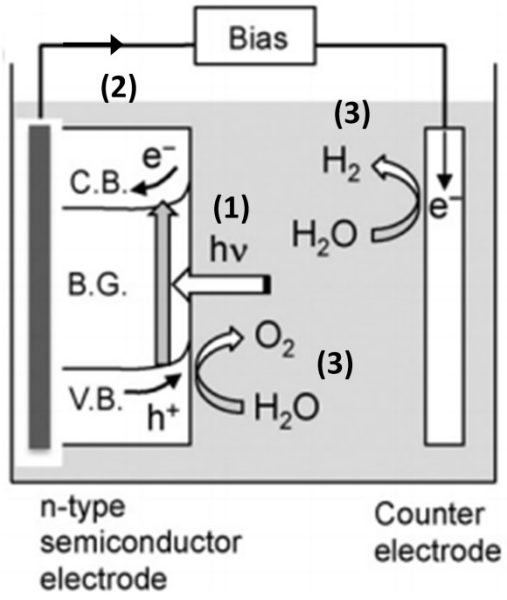

Figure 2.7 Photoelectrochemical water splitting systems using n-type semiconductor photoanode. C.B., B.G. and V.B. represent of the conductor band, band gap and valence band respectively. Source: Ref. [109].

1st: generation of electron hole pair after absorption of photons by photo-electrode.

2nd: tranportation of these photo-generated carriers to the interface of photo-electrode/electrolyte and counter electrode/electrolyte interface

3rd: Catalytic reaction with water molecules where holes (h^+) oxidize water to form O_2 at photo-electrode (equation 2.12) while electrons reduce H^+ to generate H_2 at Pt cathode (equation 2.13).

$$\text{Photo-electrode: } H_2O + 2h^+ \rightarrow 2H^+ + \frac{1}{2}O_2 \quad ; \mathrm{E}^0{}_{ox} = -1.23V \tag{2.12}$$

$$\text{Cathode} \quad : 2H^+ + 2e^- \rightarrow H_2 \quad ; \mathrm{E}^0{}_{red} = 0V \tag{2.13}$$

The performance of the water photoelectrolysis cell can be determined by the photoconversion efficiency (n) which is the efficiency to convert light energy to chemical energy with the applied potential. The photoconversion efficiency is defined as [111, 112]:

$$n = \frac{J_{photo}(1.23 - V_{bias})}{P_{light}} \times 100\% \tag{2.14}$$

where J_{photo}, V_{bias}, and P_{light} represent photocurrent density, applied potential and intensity of the light respectively.

Apart from photoconversion efficiency, the performance of the photoelectrolysis cell could also be evaluated by photon to current conversion efficiency (IPCE) which measures the efficiency to convert photon's incident on the cell to photocurrent flowing between the working and counter electrodes. The IPCE is defined as [113]:

$$IPCE = \frac{I_{ph}(\lambda)}{qP(\lambda)} \times 100\% \tag{2.15}$$

where $I_{ph}(\lambda)$ is the photocurrent density at wavelength λ; q is the electronic charge; $P(\lambda)$ is the incident photon flux densitiy of certain wavelength at the photoelectrode.